Wind Energy

WIND ENERGY
Wind Energ. 2016; **19**:1223–1237
Published online 19 August 2015 in Wiley Online Library (wileyonlinelibrary.com). DOI: 10.1002/we.1893

RESEARCH ARTICLE

Characterization of the wind speed variability and future change in the Iberian Peninsula and the Balearic Islands

Guillermo Gómez[1], William David Cabos[1], Giovanni Liguori[1], Dmitry Sein[2], Sergio Lozano-Galeana[3], Lluís Fita[4], Jesús Fernández[5], María Eugenia Magariño[5], Pedro Jiménez-Guerrero[6], Juan Pedro Montávez[6], Marta Domínguez[7], Raquel Romera[7] and Miguel Ángel Gaertner[8]

[1] Department of Physics, Climate Physics Group, University of Alcalá de Henares, Madrid 28805, Spain
[2] Alfred Wegener Institute for Polar and Marine Research, Am Handelshafen 12, Bremerhaven 27570, Germany
[3] National Renewable Energy Centre (CENER), Ciudad de la Innovación 7, Sarriguren 31621, Spain
[4] Laboratorie de Météorologie Dynamique, CNRS, UPMC-Jussieu, Paris, France
[5] Grupo de Meteorología, Department of Applied Mathematics and Computer Science, University of Cantabria, Santander 39005, Spain
[6] Department of Physics, Regional Campus of International Excellence 'Campus Mare Nostrum', University of Murcia, Murcia 30100, Spain
[7] Environmental Sciences Institute, University of Castilla La Mancha, Toledo 45071, Spain
[8] Environmental Sciences Faculty, University of Castilla La Mancha, Toledo 45071, Spain

ABSTRACT

Wind energy is susceptible to global climate change because it could alter the wind patterns. Then, improvement of our knowledge of wind field variability is crucial to optimize the use of wind resources in a given region.

Here, we quantify the effects of climate change on the surface wind speed field over the Iberian Peninsula and Balearic Islands using an ensemble of four regional climate models driven by a global climate model.

Regions of the Iberian Peninsula with coherent temporal variability in wind speed in each of the models are identified and analysed using cluster analysis. These regions are continuous in each model and exhibit a high degree of overlap across the models. The models forced by the European Reanalysis Interim (ERA-Interim) reanalysis are validated against the European Climate Assessment and Dataset wind. We find that regional models are able to simulate with reasonable skill the spatial distribution of wind speed at 10 m in the Iberian Peninsula, identifying areas with common wind variability.

Under the Special Report on Emissions Scenarios (SRES) A1B climate change scenario, the wind speed in the identified regions for 2031–2050 is up to 5% less than during the 1980–1999 control period for all models. The models also agree on the time evolution of spatially averaged wind speed in each region, showing a negative trend for all of them. These tendencies depend on the region and are significant at $p = 5\%$ or slightly more for annual trends, while seasonal trends are not significant in most of the regions and seasons. Copyright © 2015 John Wiley & Sons, Ltd.

KEYWORDS
K-means; wind speed; regional climate models; Iberian Peninsula

Correspondence
G. Gómez, Department of Physics, Climate Physics Group, University of Alcalá de Henares, Madrid 28805, Spain.
E-mail: guillermo.gomez@edu.uah.es

Received 21 October 2014; Revised 18 June 2015; Accepted 13 July 2015

1. INTRODUCTION

Presently, there is great concern about the depletion of conventional energy sources and its effects on the environment and the climate. One approach for both problems is to adopt the use of renewable energies. Among these, wind energy has been ranked first for potential to generate energy, impact on environment, reduction of greenhouse gas emissions and the

development of a high-tech industry and highly qualified jobs.[1] Because of these advantages, wind power has become an important energy source in the last decades. For instance, the European Union has set a binding target of a 20% renewable energy contribution by 2020, aiming to increase the share of electricity from wind resources to 12% by that time.[2] Spain is one of the countries that it has moved the furthest in this direction. In recent years, wind power has become an important component of energy generation, meeting 21.1% of the electrical energy demand in 2013 and making wind energy the single most important electrical energy source in this country for this year.

Although wind energy density is a cubic function of wind speed, wind turbines produce energy at a band of wind speeds (usually 3–26 ms^{-1}), and beyond a nominal wind speed, the production of wind turbines is constant making the wind potential more sensitive to changes in lower than high wind speeds.[3] Thus, decreases in wind speed could have significant consequences for power production and hence for the overall economics of wind power plant projects. This highlights the importance of accurate quantification and attribution of historical trends, and at the same time, robust projections of likely future wind resources are made.

The surface circulation of the Iberian Peninsula (IP) is controlled by the Azores High. In winter, when the subtropical high pressure is usually centered at lower latitudes, zonal circulations from the west coupled with perturbations originated by the polar front affect the IP.[4] In summer, except for the northern region, the western circulations over the IP are blocked by the Azores High expansion to higher latitudes. The displacements and changes in the intensity of the Azores High allow a variety of air masses of different origins to influence the circulation over the IP at regional and local scales. These include polar continental air masses; the Sahara Low, Arctic and Polar maritime air masses coming through the north and northwest of the peninsula, and subtropical and tropical maritime air masses coming from the west or the southwest are the most well known.[4] Additionally, air masses from the Mediterranean Sea can penetrate the IP from the east or the southeast. The interaction of this variety of air masses and a particular complex topography produces a range of differentiated regional wind climates.[5,6]

The aforementioned atmospheric circulation and pressure patterns that affect the IP climate might change under future climate conditions.[7] Under the SRES A1B scenario, an ensemble of CMIP3 global climate models projects a significant enhancement of the meridional pressure gradient over central and Western Europe, which strengthens the westerly mean flow[8] that is associated with a significant poleward shift of storm tracks to the end of the 21st century. Furthermore, Kjellström *et al.*[9] shows that mean wind speed over Europe and their seasonality may change, showing an increase of 8% in the wind velocity in Northern Europe, a decrease in the Mediterranean central area and a slight increase in Southeastern Europe. Other studies focusing on different parts of Europe have found variations in wind patterns and behavior. For example, Bloom *et al.*[10] found a decrease of the wind speed over the sea and an increase over land in the eastern Mediterranean region. Pryor *et al.*[11] show important increases in the wind power over the southeast of Scandinavian Peninsula and the Baltic Sea. Although there are no published studies of the evolution of wind energy potential under climate change focused on the IP, some recent studies of the wind evolution on the European continent show a clear but small decrease in winds over Spain (e.g. Tobin *et al.*[12]). Besides, given the importance of wind energy for Spain, several institutions have characterized with great detail the surface wind and wind energy potential over specific regions of the IP and the Canary and the Balearic Islands (BI).[5,6]

This study aims at characterizing the surface (10 m) wind speed in an ensemble of regional climate models (RCMs) simulations from the ESCENA project.[13] To meet this aim, we developed a clustering method that allows us to group into the same cluster, those points that share similar temporal wind speed behavior, identifying regions with consistent wind series in each of the models of the ensemble. We then sought equivalent clusters across all models. We evaluated the RCMs by comparing the wind speed probability density functions (PDFs) of each common region against the PDFs of the wind from all the European Climate Assessment and Dataset (ECA&D) stations located in the region and by studying the correlation between the RCMs and the ECA&D monthly wind series.

Finally, we also evaluated the changes in modeled wind speed under A1B scenario comparing the wind speed for the periods of 1980–1999 and 2031–2050 in each of the sub-regions identified from the cluster analysis.

The present paper is organized as follows. Section 2 presents the method and tools developed to study the wind speed variability. In Section 3, we validate the method and apply it to the winds simulated under present time forcing and present and discuss the results for the climate change projections under the A1B scenario. Finally, in Section 4, a short summary and conclusion completes this paper.

2. DATASET AND METHODOLOGY

2.1. Model data and observation

2.1.1. ESCENA dataset

ESCENA (http://proyectoescena.uclm.es) procures a scientific background for the use of RCMs to the study of regional climate change impacts over Spain.

A brief description of the RCMs used in the project (PROMES, MM5, REMO and WRF) and an evaluation of their performance under present climate conditions can be found in Jimenez-Guerrero *et al.*13 and Dominguez *et al.*14

The RCM domains comprise the whole IP and BI with a horizontal resolution of 25 km (Figure 1). Since the different RCMs used different domains and different grid projections, model wind was interpolated to a common $0.2 \times 0.2^{\circ}$ grid by means of the nearest neighbor algorithm, interpolating the land and the sea grid points separately. With this resolution, the RCMs are only able to reproduce the main geographical feature of the IP and BI; nevertheless, the wind speed PDFs of simulated winds compare well with observations from the ECA&D.

The simulations analysed here are focused on the near future. They cover a control period (1950–2000) forced by boundary conditions from the 20C3M ECHAM5–MPIOM historical run and the near future period 2001–2050, with boundary conditions from the second run of the ECHAM5–MPIOM A1B scenario. Additionally, perfect boundary simulations forced by the high-resolution ERA-Interim reanalysis were carried out to evaluate the RCMs. These cover the period of 1989–2008.

2.1.2. ECA&D wind speed

The ECA&D[15] is a collection of daily station time series of Europe and the Mediterranean area gathered from the National Meteorological and the Hydrological Services of the different countries. These series are subjected to complementary, common quality control procedures drawn from the ECA&D project (http: http://eca.knmi.nl).

This dataset contains more than 100 surface wind speed daily time series from stations located in the IP that cover the last half of the 20th century. The ECA&D data series, however, do not include wind data for Portugal (15% of the whole area of study), and therefore, the results of the RCMs for this area could not be validated. From the original 112 stations, we rejected those with more than 10% invalid data in the period from 1983 to 2013, resulting in 71 valid time series.

2.2. Methodology

2.2.1. Clusters analysis

Because of its complex orography and its position with respect to the north Atlantic, the IP presents extensive climate heterogeneity.[4] The region has six main mountain systems, one big central plateau and three depressions. Low-altitude winds are strongly conditioned by interactions with this complex orography, the large-scale circulation and a variety of distinct air masses of different origins that influence the circulation over the IP. This leads to very different regional patterns of wind variability in the IP.

High-resolution RCM simulations can provide better information on these spatial scales than global climate models. However, limitations in terms of process representation still prevent the interpretation of model results on single grid cells. Therefore, climate change patterns are frequently aggregated over space in order to reduce the complexity of result communication and to reinforce the robustness of the simulation results.

When it comes to model ensembles, an additional issue arises: how and on what spatial scale results from ensembles of climate models should be analysed. On the one hand, the model agreement generally increases on larger scales.[16] If a region is too small, different models may disagree in their signal. On the other hand, if the region is too large, the changes can be blurred, and information can be lost because different climate regimes are averaged together, e.g. averaging positive and negative wind change will result in little net change. One way to overcome this problem and find the proper spatial scale would be to use clustering methods.

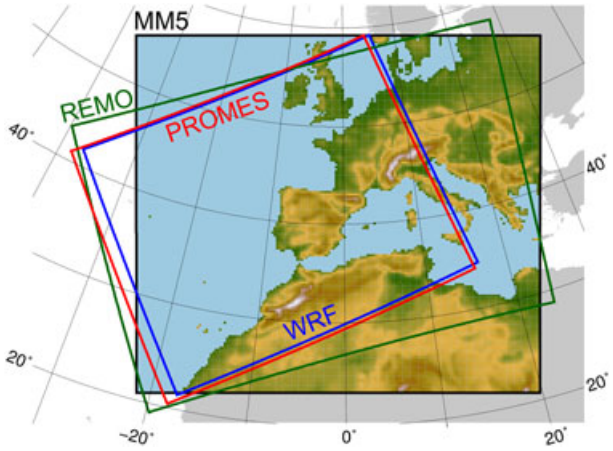

Figure 1. Simulation domain of the ESCENA RCMs.

Regional climate change results are normally presented using regions of simple shape,[17] basins or climate-type classifications.[18] But in reality, regions of similar climate are not constrained to simple shapes, and in addition, each climate variable presents different patterns of change, often not coinciding with a given basin or climate-type region. The variable(s) of interest, the current mean climate and the projected future changes should determine how the simulated climate change results are aggregated to the regions. An alternative procedure to define regions where the climate change signal is similar in some objective sense of distance for all grid cells involves the use of cluster analysis methods.[19] The hypothesis is that, in function of the variable(s) of interest, the models can provide robust information for a number of regions, reducing the degrees of freedom of the climate data.

Cluster analysis has long been recognized as a useful statistical method for grouping stations into region with similar climatology based upon given meteorological parameters. It is also useful for classifying weather conditions into different synoptic regimes,[20] partitioning a domain of interest into distinct climatic zones[21] and for model validation with sparse observations in paleoclimate studies.[22] Mahlstein and Knutti[19] devised an algorithm that allowed them to define regions with similar mean climate and projected changes for CMIP3 models. They found a significant reduction of the projected changes on different climate variables, i.e. the consistency of the mean climate and the expected changes are more robust in each region and therefore more representative of regional impacts.

Thus, cluster analysis seems to be well suited for the goal of this study: to assess in a robust way the ability of the ESCENA project models to simulate the observed wind variability when forced with perfect boundary conditions using a relatively sparse observed wind dataset and to reduce the spatial and intermodel uncertainty of the projected future changes of wind. To this end, we define criteria to divide the IP + BI into the minimum number of regions with similar wind characteristics. There are many different algorithms to classify observations or model data into clusters.[23] To identify which method fits better to our purpose, we applied centroid methods (K-means), hierarchical clustering (Ward's minimum variance), spectral clustering (SPCL) and density-based methods on the RCMs results. We found that density methods are not appropriate to this study, so they show big problems when they deal with high-dimensional data. Moreover, K-means, Ward's minimum variance and SPCL present similar results, but Ward's classifies less points in the optimal ensemble partition than the other two, and SPCL is rather sensitive to the metric, so we decided to use the conventional K-means algorithm. Using this method, the time series of daily wind speed of the grid points of the RCMs and the meteorological stations of ECA&D are grouped into disjoint regions (clusters), and the current wind climate and its projected future changes are studied using the aggregated wind characteristics in these sub-regions.

The main drawback of the K-means method is that the number of clusters must be given in advance. In addition, multiple solutions may exist, and the algorithm can become trapped in a local optimum far away from the best global solution. Thus, detecting whether a specific optimum is an actual global optimum might be impossible from a computational point of view. One strategy to overcome this difficulty is to run the algorithm multiple times varying the initial seeds of clusters, reducing the probability of converging to a local minimum of very low quality. Another drawback is that the possible heterogeneity of the simulated and measured wind speeds could produce undesirable effects if the K-means algorithm is applied directly. To deal with this problem, a principal component analysis of the data is performed, and the K-means method is then applied on these normalized principal components.[24] The application of a principal component analysis not only produces a noise reduction but also[25] proves that the continuous solution of the cluster membership indicators is given by the principal components in the K-means clustering method.

Applying this method to the simulations forced by ERA-Interim and by ECHAM5–MPIOM for each number of clusters and forcings, we obtain a set of four classifications, one for each model. The partitions in a given set can be more or less similar, but for a given forcing, it is desirable that all model partitions are as similar as possible to each other. This would mean that all models capture the same spatio-temporal wind variability and that the obtained clusters are robust across models. Therefore, the optimal number of clusters would be that, with the highest degree of similarity among all models partitions. The strategy used to identify the optimal number of clusters is explained in the following section.

2.2.2. Selection of the number of clusters

To find the optimal number of clusters, we first merge each set of four partitions into only one. The algorithm used is described as follows:

- First, the partition of one of the set members is set up as a partition of reference.
- Second, a correspondence between the clusters of the remaining models with the reference partition is established. A cluster is considered equivalent to a given cluster from the partition of reference when it shares the largest area with it.
- Third, a point is classified into a cluster of the set partition if it belongs to at least three different equivalent clusters. Some blank areas could appear in the ensemble partition if there are unclassified points.

We repeat the procedure using each model as a reference, selecting the partition that maximizes the number of classified points as the final set partition. This way, we obtain a unique partition per a given number of clusters and a forcing.

To find the number of clusters that gives the optimal ensemble partition for one of the forcings, several criteria can be used.[26] In this paper, we define a new criterion based on the following two parameters:

Compactness: We define the compactness C_K of an ensemble partition for K clusters as the mean compactness of the corresponding partitions of the ensemble members. We define the model compactness c_K for a partition of K cluster as the inverse of the spatial and temporal averages of the spatial variance of the K clusters:

$$c_K^{-1} = \frac{1}{K}\sum_{k=1}^{K}\left(\frac{1}{T}\sum_{i=1}^{T}\left(\frac{1}{n(k)}\sum_{j=1}^{n(k)}\left(x_{ij}(k)-\overline{x}_i(k)\right)^2\right)\right)$$

where K is the number of clusters in the partition, $n(k)$ is the number of elements (classified points) in cluster k, T is the total number of analysed days, $\overline{x}_i(k)$ is the mean wind speed for cluster k at day i and $x_{ij}(k)$ is the wind speed at time i and point j of the cluster k.

Similarity: As in defining the set of partitions, we used the number of common points of corresponding clusters, and we take the number of classified points as a measure of the similarity between members of a set partition.

The optimum number of clusters is defined as the number that minimizes the inverse product of compactness and similarity and gives the standard deviation per classified point. Figure 2 shows this index as a function of the number of clusters in the common partitions for the ESCENA ensemble forced by ERA-Interim and ECHAM5–MPIOM. In both cases, the global minimum is achieved for 11 clusters.

The corresponding global partitions for both sets of simulations are represented in Figure 3. We can note that they share a great resemblance. In order to quantify this similarity, we introduce a resemblance coefficient (RC) as follows:

$$RC = \frac{Common\_Area}{Total\_Area}$$

For two corresponding clusters, the *Common_Area* is the intersection area of the two clusters, and *Total_Area* is the whole area of one of the two clusters, so RC can be different for each cluster. The RC quantifies the fraction of the cluster of the one partition that is contained in the corresponding cluster of the other partition.

We calculate the RC using in the denominator the area of each of the corresponding clusters in the two ensembles. When the clusters are coincident, the two RC reach a value of 100%. In most cases, the RCs for both ensembles have values over 80% (Figure 3). The mean RCs, weighted by the cluster areas, are over 90% for both forcings. This result shows that the obtained partitions are robust and can be considered equivalent.

To validate our results, we compare the ensemble partitions with the ECA&D wind partition also obtained using the K-means method. To find the optimal number of clusters for the ECA&D wind partition, we apply the elbow criterion[27] to the relative standard deviation, which is defined by the following expression:

$$RSD = \frac{SD_1 - SD_N}{N-1}$$

The *RSD* gives the relative change of the mean standard deviation of a partition of N clusters (SD_N) when the number of clusters (N) is increased, using the mean standard deviation of a partition of one cluster (SD_1) as reference.

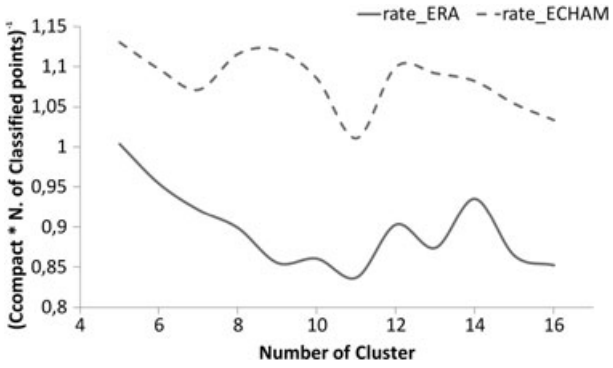

Figure 2. Selection parameter as function of the number of clusters. Solid line: simulations forced by ERA-Interim. Dashed line: simulations forced by present time ECHAM5–MPIOM. For both ensembles, the parameter reaches a minimum for 11 clusters.

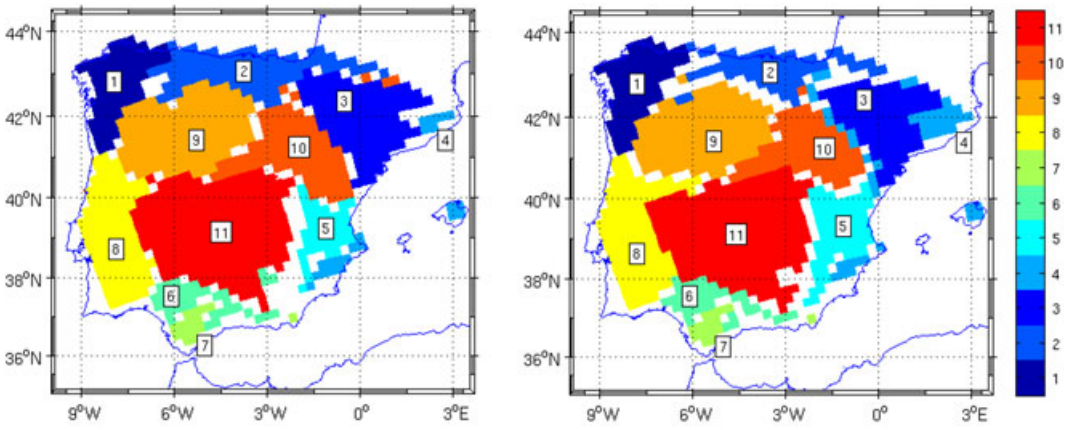

Cluster	1	2	3	4	5	6	7	8	9	10	11	mean
ECHAM5	0.97	1.00	1.00	0.40	0.65	0.92	1.00	0.92	0.97	0.97	0.97	0.91
ERA	1.00	0.70	0.82	0.82	1.00	0.89	1.00	0.96	0.93	0.81	0.97	0.90

Figure 3. Left panel: ERA-Interim partition as a result of applying K-means on RCMs results forced by ERA-Interim. Right panel: ECHAM5–MPIOM partition as a result of applying K-means on RCMs results forced by ECHAM5–MPIOM. Lower panel: resemblance coefficient between the two partitions.

Figure 4 shows that the *RSD* presents an elbow for nine clusters. The resulting nine clusters partitioning of the IP for ECA&D winds are presented in Figure 5.

Since the ECA&D clustering was obtained from 71 scattered meteorological stations, the results may be strongly influenced by local geographical features, and therefore, we cannot make a straightforward comparison between ECA&D and ensemble partitions. Because of this, in regions of complex orography, neighboring stations can belong to different clusters, for example, clusters 5 and 10 (Figures 3 and 5). On the other hand, model data represent the mean wind speed in a grid cell, and the effects of smoothed orography are less important.

Nevertheless, some qualitative relationships between ECA&D partition (Figure 5) and ERA-Interim and ECHAM5–MPIOM partitions (Figure 3) can be found. In regions of smooth orography, the stations tend to belong to the same cluster, and a correspondence between the ECA&D and both ERA-Interim and ECHAM5 model partitions can be established.

Another remarkable result from the cluster selection process is that the optimal number of clusters for ECA&D is nine, which is close to the ensemble optimum of 11 wind speed clusters for the IP and BI, even though both optimal numbers were obtained by different methods.

3. RESULTS

To evaluate the ability of RCMs to simulate the present time surface wind speed, we calculate the correlations between RCMs and ECA&D monthly wind data series and define a skill score based on the PDFs of the modeled and observed data.

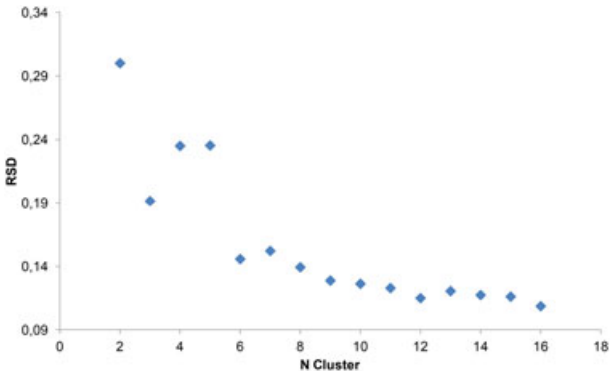

Figure 4. Relative standard deviation as function of the number of clusters for ECAD&D surface wind.

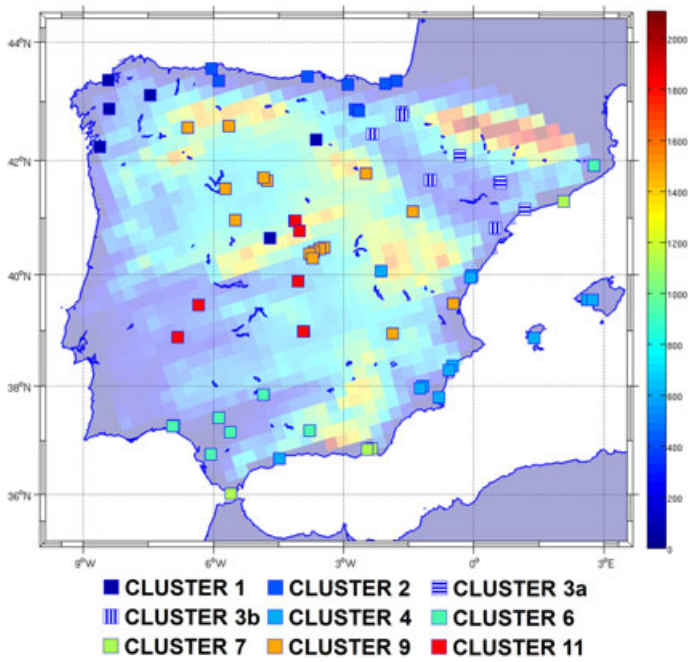

Figure 5. Classification of ECA&D stations. The numbering is in correspondence with ERA-Interim and ECHAM5–MPIOM clusters. For this correspondence, we merged two clusters of the original classification into cluster 3.

The PDFs were constructed with daily data series of the wind speed. The use of entire PDFs provides a more complete evaluation of climate models as changes in parts of the distribution, which are not the mean, can be important for impact studies, and there is evidence that extremes may be even more relevant than changes in the mean.[28] From the point of view of the wind energy industry, this is a crucial point since wind turbines usually work in a determined range of wind velocities, and changes in the frequency of weak or strong wind episodes could increase the idle periods for wind farms. Furthermore, daily data can show biases or systematic errors that can be hidden in monthly, seasonal or longer averages. Higher frequencies and resolution could show gusts or extreme events, but these phenomena are very local and brief, so their effects would be blurred in the wind speed PDF of regions of several hundreds of square kilometers, and if a model is able to simulate with good accuracy the PDF, we can be confident that the models are able to capture the observed climate variability. After the evaluation of the ability of RCMs to simulate the present time wind speed, we study evolution of the wind speed in the near future.

3.1. RCMs skill in reproducing wind speed

Before focusing on the projections of the surface wind speed in the IP and BI, we evaluate the ability of ESCENA's RCMs to simulate the surface wind speed for the area of study when either ERA-Interim or ECHAM5–MPIOM is used as boundary conditions.

As stated previously, our validation is based on correlation analysis and on a skill score derived from the probability distribution functions of the daily wind speed. The correlation analysis was only applied to RCMs forced by ERA-Interim because simulations forced by ECHAM5–MPIOM are expected to reproduce with acceptable accuracy the statistical characteristics of the observed wind but not their time evolution, since internal model variability dominates these time scales.

The number of ECA&D stations is significantly smaller than the number of the model points, so for the calculation of wind time series in the partitions, we first interpolate model data to the station locations and then calculate the spatial mean in each cluster for observed and interpolated data, obtaining a time series representative of the wind in the cluster. This way, the cluster means for observed and modeled data are based on the same number of values and represent values in the same geographical location. We used these constructed cluster means to compute the time correlations between observations and simulations forced by ERA-Interim (Table I). These correlations are always significant at 95% confidence levels and, in most of cases, are above 0.5, which for wind reproduction is a reasonable value. In addition, RCMs are able to reproduce well the PDF of observed wind speed.

The foregoing correlation analysis reveals a generally good agreement between monthly mean time series of ERA-Interim forced model and observational data. However, the analysis of high frequencies is crucial if one wants to assess

Table I. Correlation coefficients between ERA-Interim-forced simulations and ECA&D monthly time series for the 1989–2008 period.

Cluster	1	2	3	4	5	6	7	9	10	11
PROM	**0.63**	**0.65**	**0.65**	**0.25**	**0.51**	**0.42**	**0.60**	**0.79**	**0.62**	**0.75**
WRF	**0.51**	**0.64**	**0.63**	**0.27**	**0.50**	**0.32**	**0.62**	**0.77**	**0.62**	**0.69**
MM5	**0.65**	**0.68**	**0.75**	**0.35**	**0.51**	**0.43**	**0.63**	**0.79**	**0.63**	**0.77**
REMO	**0.59**	**0.67**	**0.55**	**0.36**	**0.44**	**0.37**	**0.60**	**0.77**	**0.58**	**0.69**

Correlations with a 95% confidence level are in bold.

the ensemble capability reproducing the wind power potential. Moreover, the correlation analysis cannot reveal systematic biases in mean value. For both reasons, we decided to analyse the PDFs of daily winds with the help of the Perkins skill score, defined as S_{score}, allowing us to find the common area of both distributions.[29] If a model reproduces the observed winds perfectly, the two PDFs are coincident, and the skill score will be equal to one, or 100 if it is expressed as a percentage. Therefore, we use this index as a measure of similarity between model PDFs and ECA&D PDF in a given cluster.

$$S_{score} = \sum_{1}^{n} minimum(Z_m, Z_0)$$

where n is the number of bins into which the PDF was divided, Z_m is the frequency of values of 10 m wind in a given bin from the model and Z_0 is the frequency of values of 10 m wind in the same bin from the ECA&D data.

To compare the PDFs of modeled and observed wind speed, we first interpolate daily model data to the station locations. Then the PDFs of both observed and interpolated data in each cluster are aggregated. The aggregated PDF of the observed wind is not evaluated for cluster number 8 for both ECHAM–MPIOM and ERA-Interim partitions because it does not contain any meteorological stations.

To have a quantitative measure of how close the PDFs of the models are in each cluster, we introduce the cluster dispersion (Disp). In this case, the aggregated PDFs are built from the daily winds at all the points in a cluster. This metric provides the mean deviation of the PDFs of the models in a cluster for the case when all the models have the same distribution and is defined as follows:

$$Disp = \frac{Maximum\_Area - 1}{N_m - 1}$$

where *Maximum_Area* is the area under the envelope of all models' PDFs for a cluster and is equal to one when the models have the same PDF, and N_m is the number of models in the ensemble (in this case, 4). The denominator is chosen to normalize Disp to one.

Figure 6 shows the probability wind distributions in clusters with odd numbers for the ensemble forced by the ERA-Interim. The RCMs tend to show a higher probability of strong winds than ECA&D, with REMO being closer to observations. The probability of strong winds for WRF is higher than for the other models. PROMES and MM5 show an intermediate behavior, with a similar right shift of the PDFs. The values of the S_{score} are shown in Table II. Despite differences in PDFs, RCMs show a mean skill score of 75% for both partitions with values between 51% and 95% across models and clusters. To check the similarity of the ensemble partitions for both forcings, we repeat the calculations using the partition obtained with the ensemble forced by ECHAM5–MPIOM. We obtained very similar results for both partitions.

Table III shows the cluster dispersion for the present time simulations forced by ERA-Interim. It is not higher than 15% for any cluster, and the mean maximum area is 30% higher than the optimum area. This implies that the models not only agree in the spatial distribution of surface winds but also share more than 85% of the PDFs in each of the clusters, pointing to a high accordance between the models in the simulation of surface winds.

3.2. Surface wind speed change (1980–1999 to 2031–2050)

As stated previously, simulations of current climate with the RCMs forced by ECHAM5–MPIOM give results similar to those obtained in simulations forced by ERA-Interim. This is probably an indication that the differences in winds simulated by the ESCENA models depend weakly on the forcing. This conclusion is reinforced by comparing metrics in Tables II and III with the corresponding Tables IV and V. The skill scores of clusters corresponding to the simulations forced by ECHAM5–MPIOM are similar to the skill scores of the RCMs forced by ERA-Interim, being clearly worse only for clusters 9 and 10. The cluster dispersion is also very similar for both partitions, with close values for all clusters.

We have also calculated the values of the cluster dispersion for the period of 2031–2050 in the A1B scenario simulations. The cluster dispersion for this period for all the clusters is also similar to the values obtained for the ensemble

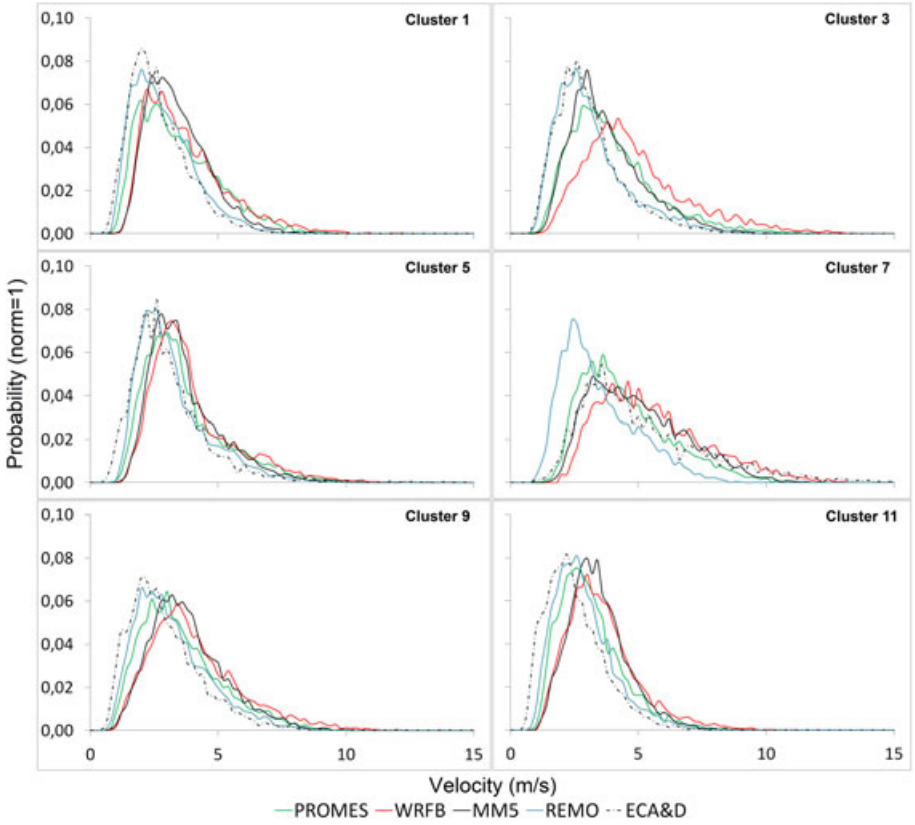

Figure 6. Probability distribution functions of daily surface wind speed for ECA&D and ERA-Interim-forced simulations for the 1989–2008 period.

Table II. Skill score (in %) of surface wind PDFs for ESCENA RCMs forced by ERA-Interim (1989–2008 period) for corresponding partition.

Cluster	1	2	3	4	5	6	7	8	9	10	11	Mean
PROMES	79	68	76	68	81	93	88	—	82	72	78	78
WRF	72	62	56	51	71	83	84	—	69	57	65	65
MM5	72	69	78	65	75	57	88	—	71	61	64	68
REMO	92	89	95	90	91	78	68	—	91	85	86	88
Mean	79	72	76	69	80	78	82	—	78	69	73	75

Table III. Dispersion of the surface wind PDFs for the ESCENA RCMs forced by ERA-Interim (1989–2008 period) for the corresponding partition.

Cluster	1	2	3	4	5	6	7	8	9	10	11	Mean
Maximum area	1.28	1.36	1.38	1.40	1.28	1.36	1.31	1.30	1.25	1.29	1.27	1.30
Disp (%)	9	12	13	13	9	12	10	10	8	10	9	10

partition of the simulations forced by ERA-Interim. This indicates that the RCMs maintain a good agreement in the statistical characteristics of future simulated wind distributions (Table VI).

The relative changes in the mean wind for the 2031–2050 period under the A1B scenario with respect to the control period (1980–1999) for each model and cluster are presented in Table VII. All the models show negative changes in the 11 clusters. For each model, the absolute changes that are smaller than the mean for all clusters are marked in light gray, while the changes greater than the mean are marked in gray; it can be seen that although the models differ in the magnitude of the

Table IV. Skill score (in %) of surface wind PDFs for ESCENA RCMs forced by ECHAM5–MPIOM (1980–1999 period) for clusters of the corresponding partition.

Cluster	1	2	3	4	5	6	7	8	9	10	11	Mean
PROMES	78	62	75	58	88	91	87	—	76	67	71	74
WRF	76	56	59	46	81	81	86	—	66	55	59	64
MM5	73	61	77	56	84	85	87	—	66	56	59	67
REMO	93	85	93	91	90	79	66	—	85	79	81	85
Mean	80	66	76	63	86	84	82	—	73	64	68	72

Table V. Cluster dispersion of the surface wind PDFs for ESCENA RCMs forced by ECHAM5–MPIOM (1980–1999 period) for clusters of the corresponding partition.

Cluster	1	2	3	4	5	6	7	8	9	10	11	Mean
Maximum area	1.28	1.37	1.42	1.42	1.31	1.37	1.34	1.31	1.26	1.28	1.28	1.31
Disp (%)	9	12	14	14	10	12	11	10	9	9	9	10

Table VI. Cluster dispersion of the surface wind PDFs for ESCENA RCMs for 2031–2050 in the partition from present time simulations forced by ECHAM5–MPIOM.

Cluster	1	2	3	4	5	6	7	8	9	10	11	Mean
Maximum area	1.27	1.37	1.41	1.41	1.30	1.37	1.34	1.30	1.26	1.28	1.27	1.31
Disp (%)	9	12	14	14	10	12	11	10	9	9	9	10

Table VII. Changes in mean wind speed between the 2031–2050 and the 1980–1999 periods for the ESCENA models in the 11 clusters and the mean for the region of study (IP + BI).

%	PROMES	WRF	MM5	REMO	Mean
Cluster1	-1.0	-0.6	-1.2	-1.1	-1.0±0.3
Cluster2	-1.2	-1.2	-1.7	-1.4	-1.4±0.2
Cluster3	-1.3	-2.2	-2.9	-1.6	-2.0±0.7
Cluster4	-1.5	-2.0	-2.7	-2.2	-2.1±0.5
Cluster5	-2.0	-3.4	-3.1	-3.2	-2.9±0.6
Cluster6	-0.8	-1.6	-1.6	-1.0	-1.2±0.4
Cluster7	-0.0	-0.2	-0.2	-0.0	-0.1±0.1
Cluster8	-1.6	-1.6	-1.9	-1.6	-1.7±0.2
Cluster9	-1.4	-2.3	-2.5	-1.9	-2.0±0.5
Cluster10	-1.8	-2.2	-2.7	-2.6	-2.3±0.4
Cluster11	-1.5	-2.4	-2.4	-2.0	-2.1±0.4
IP+BI	-1.3	-1.8	-2.1	-1.7	-1.7±0.3

Changes less than the IP + BI mean are marked in light. Changes greater than the mean are marked in gray.

changes, they agree in the identification of those regions where the changes will be higher or lower than the mean change, with the exception of clusters 3 and 8, for which at least one model shows changes on different sides of the mean.

Figure 7 shows the spatial distribution of the regions where the relative changes in the mean wind speed for the 2031–2050 period with respect to 1980–1999 are bigger (gray) or lower (light gray) than the mean change for the whole IP and BI. We can see that the regions with smaller changes are located in the Atlantic Fringe and the southern tip of the IP, under the direct influence of the Atlantic flow, while the regions with stronger changes are located in the interior regions or in the Mediterranean fringe, where the influence of the Atlantic ocean on the winds is less important. These regional features could be related to changes in synoptic-scale circulation in a future climate.[30]

Wind Energ. 2016; **19**:1223–1237 © 2015 John Wiley & Sons, Ltd.
DOI: 10.1002/we

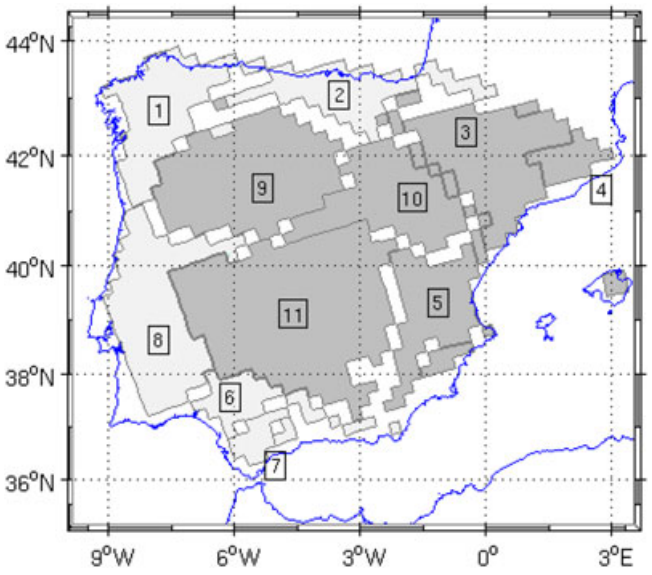

Figure 7. Spatial distribution of changes in the mean wind speed for the 2030–2050 period with respect to 1980–2000 in IP + BI. Absolute changes are less than the mean change for IP + BI in the light gray areas and higher in the gray areas.

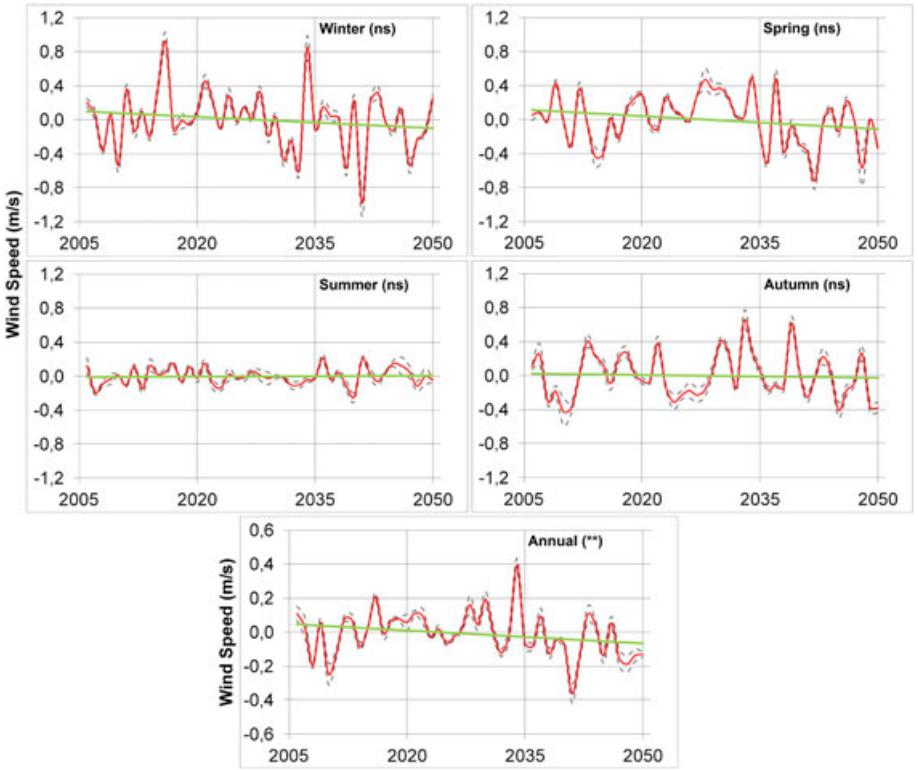

Figure 8. Time evolution of the annual and seasonal mean wind speed over the Iberian Peninsula and Balearic Islands. The red line represents the ensemble mean. Gray lines represent the model spread, and the green lines are a linear fit to the ensemble mean. The mean value for the whole period has been removed from each of the model time series. Trends marked with ns are non-significant, marked with * are significant at 10% level with a Mann–Kendall test and marked with ** are significant at 5% level with a Mann–Kendall test.

Table VIII. Trend of the surface wind speed trend (mm s^{-1} $year^{-1}$) for the 2000–2050 period for the ESCENA ensemble mean in the ensemble clusters.

	Winter	Spring	Summer	Autumn	Year
Cluster 1	−1.4	−3.3	−1.2*	−1.4	−1.8*
Cluster 2	−4.5	−5.1	−1.9	−2.0	−3.4**
Cluster 3	−8.5**	−6.5**	−0.1	−0.2	−3.8**
Cluster 4	−6.6	−2.8	0.6	−1.9	−2.7**
Cluster 5	−7.6	−5.4	2.1	−3.9	−3.7**
Cluster 6	−2.0	−4.2*	−2.2*	−2.0	−2.6**
Cluster 7	4.4	0.6	−12.9**	1.1	−1.7*
Cluster 8	−2.6	−6.4**	3.3*	−0.4	−1.5*
Cluster 9	−4.0	−3.9	0.2	−0.9	−2.4**
Cluster 10	−7.1*	−5.9	1.7	−1.6	−3.2**
Cluster 11	−1.4	−3.3	−1.2*	−1.4	−1.8*
IP + BI	−4.5	−5.1	−1.9	−2.0	−3.4**

*Trends are significant at 10% level with a Mann–Kendall test.
**Trends are significant at 5% level with a Mann–Kendall test.

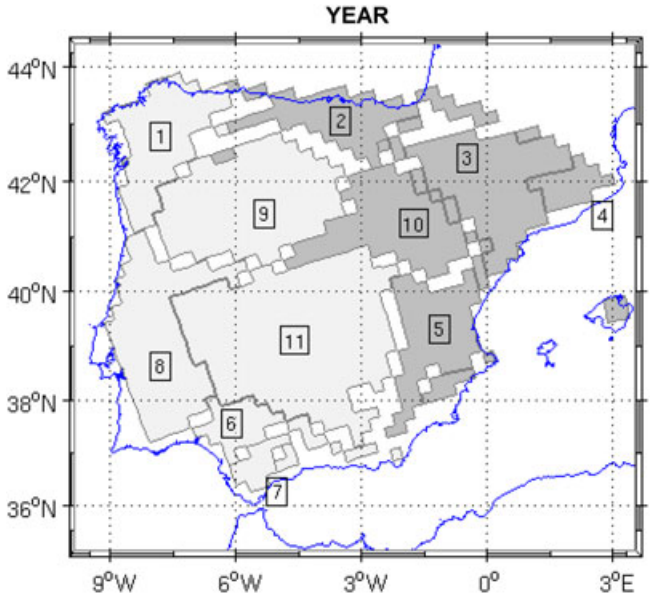

Figure 9. Spatial distribution of trends of annual mean surface wind in the IP and BI for the 2005–2050 period. Absolute trends are less than the mean trend for IP + BI in the light gray areas and higher in the gray areas. All trends are significant at a 10% level with a Mann–Kendall test.

3.3. Wind speed interannual evolution

Although the mean magnitude of the surface wind in the IP and BI varies from model to model, the tendencies of the simulated wind are very similar. In Figure 8, we represent the temporal evolution of the IP + BI mean seasonal and annual surface wind for the ESCENA ensemble after removing the mean for the whole 2005–2050 period for each model. We can see that the model spread is small for all seasons and that the models show a similar pattern of temporal evolution. The time series of ensemble-mean surface wind in IP + BI show trends that are weakly positive for the summer and negative for the other seasons, with stronger values for winter and spring. To analyse the significance of the trends, we use the Mann–Kendall test, which is especially suitable to study time series that are composed of values that are non-normally distributed, and present non-linear trends as surface winds do. For the ensemble-mean seasonal time series, the Mann–Kendall (e.g. Mavromatis and Stathis[31]) test shows that the trends are not significant.

A more detailed analysis of the time evolution of the surface wind in the IP and the BI is presented in Table VIII, where the trends of the annual and seasonal means for each cluster and the whole IP + BI domain are collected. This analysis

Wind Energ. 2016; **19**:1223–1237 © 2015 John Wiley & Sons, Ltd.
DOI: 10.1002/we

shows that the southern tip of the IP (cluster 7) displays opposite trends to most of the other clusters for all seasons, with a strong negative trend in summer. Another interesting result is that while the trends of the annual time series show a level of significance (p-value) of 0.05 for all clusters except for clusters 1 (0.10), 7 (0.09) and 8 (0.06), this does not happen for seasonal values, where, in most of the cases, the significance level is higher than 0.10—that is, the addition of seasonal data with trends, which are mainly non-significant, results in annual time series with significant decreasing trends. This could mean that when we calculate the annual mean, the negative trends reinforce each other, counteracting the possible positive trends and smoothing the variability. This enhances the signal/noise ratio, resulting in a significant negative annual trend. In Figure 9, we mark with light gray the clusters where the trend of the annual time series is less negative than the trend of annual mean surface wind speed for the whole IP + BI, while the rest of the clusters with a trend more negative than the trend of annual mean for IP + BI is gray. A clear west–east contrast can be appreciated. The regions on the western side of the IP, most affected by western Atlantic winds, show in general a less negative trend than the rest of the IP and BI.

4. DISCUSSION

In this paper, we study the evolution, from present time to 2050, of wind speed in the IP and the BI with a newly developed method based on cluster analysis. This method allowed us to identify areas of similar surface wind variability in the region of study. Our method is applied to two sets of simulations produced in the framework of the ESCENA project, one forced by ERA-Interim and a second forced by present time simulation with the general circulation model ECHAM5–MPIOM. In each case, the region of study has been divided into two partitions of 11 clusters. The two obtained partitions show very similar spatial distribution, and in most cases, two equivalent sub-regions share more than 90% of points. This demonstrates that the proposed method provides a robust spatial classification, which is mostly independent of the forcing used.

For the validation of the surface winds simulated by the RCMs, we use the ECA&D database. One of the problems that we face in the validation procedure is that the number of meteorological stations available in a given cluster is in general much lower than the number of model grid points in that region. In addition, surface winds can be heavily affected by the orography. We overcome this difficulty by calculating the probability distribution function in a cluster using model data interpolated to station locations. The PDF skill score calculated from the simulations forced by ERA-Interim and ECA&D wind data has a mean value of 75%. The skill score for the simulations forced by ECHAM5–MPIOM for the control period is slightly worse, 72%. To test the robustness of the obtained partitions, we also calculate the skill score for the winds from the ERA-Interim-forced simulations on the partition obtained with the present time simulations forced by ECHAM5–MPIOM and vice versa, obtaining values of the skill score very close to those obtained in the previous cases. These results suggest that internal variability for regional models in the IP is strongly influenced by the local orography and the impact of the external forcing on the statistical characteristics of the surface wind is almost marginal.

The closeness of the skill score values indicates that the winds in the control simulations forced by ECHAM5–MPIOM are reasonably accurate, giving confidence to the projections of future changes of the surface wind simulated by the ESCENA RCMs under the Intergovernmental Panel on Climate Change A1B scenario when we use as boundary conditions the output of the ECHAM5–MPIOM simulation.

The correlation coefficients between corresponding observed and modeled surface wind velocity in the clusters have a mean value of 0.65 and in all clusters are significant to the 95% confidence level. The RCMs wind data series used for the correlations were obtained by interpolation to the station locations, giving, as a result for each cluster, the same number of time series for the RCMs and for ECA&D.

A subjective validation of the previous results can also be made, based on the wind climatology of the IP + BI. It is well known that dominant near-surface winds are strongly forced by topography and pressure contrasts between land and sea. In addition, there is a well-defined periodic seasonal cycle. On the other hand, the mountainous terrain that surrounds the flat plains of the IP has a marked influence on the movement of air masses over the IP. Examining the clusters represented in Figure 3, it is easy to identify them with specific geographic regions like the Ebro Valley. This valley is characterized by the cierzo wind, which is a west–northeast wind component blowing to east–southeast or its opposite throughout the entire year. Cierzo is originated by the pressure gradient between the Cantabrian and Mediterranean seas and is channeled through this valley. Cluster 3 perfectly represents the region affected by this wind pattern. Cluster 1 can be related to the Galicia region, which is affected by West winds coming from Atlantic low-pressure systems. This wind is blocked by the Leon Mountains and the Cantabrian mountain range clearly distinguishing Galicia (cluster 1) from the Castilian plateau (cluster 9). The Castilian plateau is also separated by the Cantabrian mountain range from the north coast of Spain (cluster 2), which is under the influence of north winds or south winds. These conditions help to create the Foehn effects characteristic of the Cantabrian region. The Levante wind originates in the central Mediterranean Sea and affects the east coast (cluster 5) inducing severe rain events in the east coast during autumn season. The Strait of Gibraltar, located at the western entrance to the Mediterranean Sea, is characterized by strong gap winds. It is a narrow 15 km wide and 55 km long sea-level passage surrounded by high mountains (the Atlas Mountains in Morocco and the Betic range in Spain). Cluster 7 is clearly related to this region. Cluster 6 is identified with the Guadalquivir valley. This is an open basin where wind with a SW component is

forced by the pressure systems on the Gulf of Cadiz. This analysis shows that there is a great deal of correspondence between known surface wind geographical features and those obtained from our cluster classification as obtained by Lorente-Plazas *et al*.5,6. Regions with a simpler orography (cluster 1 or 2) have a stronger correspondence than regions with a complex orography (cluster 5 or 10).

To study the wind speed evolution in the IP and BI in the A1B scenario, we perform two different statistical analyses.

First, we compare wind climatologies for the 1980–1999 and 2031–2050 periods, obtaining a generalized decrease of the mean wind speed in the entirety of the IP and BI. This decrease is more marked for clusters that do not belong to the Atlantic Fringe. The only exception is cluster 7, which covers the southern tip of the IP and where the highest mean winds can be found for both models and observations. This region shows a negligible reduction in its mean wind speed.

Second, we study the time evolution of annual averages for the 2005–2050 period, finding negative trends for all clusters. The values of these trends are comprised between $1.5 \cdot 10^{-3}\,\mathrm{ms}^{-1}\,\mathrm{year}^{-1}$ for cluster 8 and $3.8 \cdot 10^{-3}\,\mathrm{ms}^{-1}\,\mathrm{year}^{-1}$ for cluster 3, which means a decrease of less than 5% by 2050 for any region of the IP + BI. The trends in the identified clusters show a seasonal dependence, for example, in summer, there are several clusters with slightly positive trends. Cluster 7 shows an opposite behavior to the majority of the other clusters with a positive trend for all seasons except for summer. This summer wind reduction might be due to a displacement of the Azores high, leading to weaker easterly winds over Gibraltar strait. The majority of the seasonal trends are not significant at the 0.10 level, while most of the annual trends are significant at the 0.05 level. The spatial distribution of the trends—presented in Figure 9—shows clearly a west–east contrast: the winds in the western clusters present smaller trends than the eastern clusters. This fact could be explained by the higher influence of the western Atlantic Ocean climate on these regions.

It is also noteworthy that despite the differences in the strength of the mean simulated wind, the model spread of the IP + BI trends is less than 5% for the seasonal and annual time series, showing that the RCMs of the ESCENA ensemble agree in the simulation of the trends.

The results presented here may be sensitive to the horizontal grid resolution, the scenarios and the RCM used for the simulations and the quality of wind measurements. Nevertheless, the tendencies in the evolution of wind speed in the IP under the A1B scenario identified in our paper seem to be common to all RCMs tested. Therefore, we think that it is important to continue the study of the evolution of the wind in this region with our newly developed methodology, considering different Intergovernmental Panel on Climate Change scenarios and/or different ensembles of RCMs as ENSEMBLES and EURO-CORDEX.

ACKNOWLEDGEMENT

We thank Timothy Petliar and Arturo Quintanar for helping to improve our manuscript. The Spanish Ministerio de Medio ambiente y Medio Rural y Marino funded this research through project ESCENA (ref: 200800050084265). REMO results (from UAH) were obtained through the Spanish project CGL2008-05112-C02-02. Project CGL2010-18013, financed by the Spanish Ministerio de Economía y Competitividad, also contributed to this study.

REFERENCES

1. Jacobson M. Review of solutions to global warming, air pollution, and energy security. *Energy & Environmental Science* 2009; **2**: 148–173.
2. EWEA. Pure power – wind energy scenarios up to 2030. European Wind Energy Association, Brussels (European Wind Energy Association) 2008. [Online]. Available: http://www.ewea.org.
3. Manwell JF, McGrown JG, Rogers AL. Wind Energy Explained, Theory, Design and Application (2nd edn). Wiley: Chichester, 2009.
4. Font-Tullot I. Climatología de España y Portugal (2a edición). Ediciones Universidad de Salamanca: Salamanca, 2000.
5. Lorente-Plazas R, Montávez JP, Jimenez PA, Jerez S, Gómez-Navarro JJ, García-Valero JA, Jiménez-Guerrero P. Characterization of surface winds over the Iberian Peninsula. *International Journal of Climatology* 2014. DOI: 10.1002/joc.4034.
6. Lorente-Plazas R, Montávez JP, Jerez S, Gómez-Navarro JJ, Jiménez-Guerrero P, Jiménez PA. A 49 year hindcast of surface wind over the Iberian Peninsula. *International Journal of Climatology* 2014. DOI: 10.1002/joc.4189.
7. Demuzere M, Werner M, van Lipzig NPM, Roeckner E. An analysis of present and future ECHAM5 pressure fields using a classification of circulation patterns. *International Journal of Climatology* 2009; **29**: 1796–1810.
8. Field CB, Barros VR, Dokken DJ, Mach KJ, Mastrandrea MD, Bilir TE, Chatterjee M, Ebi KL, Estrada YO, Genova RC, Girma B, Kissel ES, Levy AN, MacCracken S, Mastrandrea PR, White LL. Climate change 2014 impacts,

adaptation, and vulnerability. Part A: global and sectoral aspects. Working Group II to the Fifth Assessment Report of the Intergovernmental Panel on Climate Change, 2014.
9. Kjellström E, Nikulin G, Hansson U, Strandberg G, Ullerstig A. 21st Century changes in the European climate: uncertainties derived from an ensemble of regional climate model simulations. *Tellus A* 2011; **63**: 24–40.
10. Bloom A, Kotroni V, Lagauvardos K. Climate change impact of wind energy availability in the Eastern Mediterranean using the regional climate model PRECIS. *Natural Hazards and Earth System Sciences* 2008; **8**: 1249–1257.
11. Pryor SC, Barthelmie RJ, Kjellstromr E. Analyses of the potential climate change impact on wind energy resources in northern Europe using output from a Regional Climate Model. *Climate Dynamics* 2005; **25**: 815–835.
12. Tobin I, Vautard R, Balog I, Bréon FM, Jerez S, Ruti PM, Thais F, Vrac M, Yiou P. Assessing climate change impacts on European wind energy from ENSEMBLES high-resolution climate projections. *Climatic Change* 2015; **128**: 99–112. DOI: 10.1007/s10584-014-1291-0.
13. Jimenez-Guerrero P, Montavez JP, Domínguez M, Romera R, Fernandes J, Liguori G, Cabos Narvaez W, Gaertner MA. Description of mean fields and interannual variability in an ensemble of RCM evaluation simulations over Spain: results from the ESCENA project. *Climate Research* 2013. ISSN: 0936-577X.
14. Dominguez M, Romera R, Sanchez E, Fita L, Fernandez J, Jimenez-Guerrero P, Montalvo JP, Cabos WD, Liguori G, Gaertner MA. Precipitation and temperature extremes under present climate over Spain from a set of high resolution RCMs. *Climate Research* 2013; **58**: 149–164. DOI: 10.3354/cr01186.
15. Klein Tank AMG, Coauthors. Daily dataset of 20th-century surface air temperature and precipitation series for the European Climate Assessment. *International Journal of Climatology* 2002; **22**: 1441–1453.
16. Räisänen J. How reliable are climate models? Department of Physical Sciences, Division of Atmospheric Sciences, P. O. Box 64, FIN-00014 University of Helsinki, Finland, 2007.
17. Giorgi F, Mearns LO. Probability of regional climate change based on the reliability ensemble averaging (REA) method. *Geophysical Research Letters* 2003; **30**: 1629. DOI: 10.1029/2003GL017130.
18. Jacob D, Elizalde A, Haensler A, Hagemann S, Kumar P, Podzun R, Rechid D, Remedio AR, Saeed F, Sieck K, Teichmann C, Wilhelm C. Assessing the transferability of the regional climate model REMO to different coordinated regional climate downscaling experiment (CORDEX) regions. *Atmosphere* 2012; **3**: 181–199.
19. Mahlstein I, Knutti R. Regional climate change patterns identified by cluster analysis. *Climate Dynamics* 2010; **35**: 587–600.
20. Peña JC, Aran M, Cunillera J, Amaro J. Atmospheric circulation patterns associated with strong wind events in Catalonia. *Natural Hazards and Earth System Sciences* 2011; **11**: 145–155. DOI: 10.5194/nhess-11-145-2011.
21. Lund R, Li B. Revisiting climate region definitions via clustering. *Journal of Climate* 2009; **22**: 1787–1800. DOI: 10.1175/2008JCLI2455.1.
22. Brewer S, Guiot J, Torre F. Mid-Holocene climate change in Europe: a data-model comparison. *Climate of the Past* 2007; **3**: 499–512.
23. Jain AK, Murty MN, Flynn PJ. Data clustering: a review. *ACM Computing Surveys* 1999; **31**: 264–323.
24. Vallée F, Brunieau G, Pirlot M, Deblecker O, Lobry J. Optimal wind clustering methodology for adequacy evaluation in system generation studies using nonsequential Monte Carlo simulation. *IEE Transactions on Power Systems* 2011; **26**: 2173–2184.
25. Ding C, He X. K-means clustering via principal components analysis. *Proceedings of the 21st International Conference on Machine Learning*, Banff, Canada, 2004.
26. Rokach L, Maimon O. Chapter 15 clustering methods. In Data Mining and Knowledge Discovery Handbook, Department of Industrial Engineering Tel-Aviv University. Springer, 2013. ISBN: 13978-0-387-24435-8.
27. Thorndike RL. Who belong in the family? *Psychometrika* 1953; **18**: 267–276.
28. Schaeffer M, Selten FM, Opsteegh JD. Shifts in means are not a proxy for changes in extreme winter temperatures in climate projections. *Climate Dynamics* 2005; **25**: 51–63.
29. Perkins SE, Pitman AJ, Holbrook NJ, McAneney J. Evaluation of the AR4 climate models' simulated daily maximum temperature, minimum temperature, and precipitation over Australia using probability density functions. *Journal of Climate* 2007. DOI: 10.1175/JCLI4253.1.
30. Santos JA, Rochinha C, Liberato MLR, Reyes M, Pinto JG. Projected changes in wind energy potentials over Iberia. *Renewable Energy* 2015; **75**: 68–80.
31. Mavromatis T, Stathis D. Response of the water balance in Greece to temperature and precipitation trends. *Theoretical and Applied Climatology* 2011; **104**: 13–24. DOI: 10.1007/s00704-010-0320-9.